



# Investigation of Al-hydroxide Precipitate Fouling on the Nanofiltration Membrane System with Coagulation Pretreatment: Effect of Inorganic Compound, Organic Compound, and Their Combination

Yang Hun Choi, Ji Hyang Kweon<sup>†</sup>

Department of Environmental Engineering, Konkuk University, Seoul 143-701, Korea

## Abstract

Nanofiltration (NF) experiments were conducted to investigate fouling of Al-hydroxide precipitate and the influence of organic compound, inorganic compound, and their combination, i.e., multiple foulants.  $\text{CaCl}_2$  and  $\text{MgSO}_4$  were employed as surrogates of inorganic compounds while humic acid was used as surrogate of organic compound. The flux attained from NF experiments was fitted with the mathematical fouling model to evaluate the potential fouling mechanisms. Al-hydroxide fouling with a cake formation mechanism had little effect on the NF membrane fouling regardless of the Al concentration. The NF fouling by Al-hydroxide precipitate was deteriorated in presence of inorganic matter. The effect of Mg was more critical in increasing the fouling than Ca. This is because the Mg ions enhanced the resistances of the cake layer accumulated by the Al-hydroxide precipitate on the membrane surfaces. However, the fouling with Mg was dramatically mitigated by adding humic acid. It is interesting to observe that the removal of the conductivity was enhanced to 61.2% in presence of Mg and humic acid from 30.9% with Al-hydroxide alone. The influence of dissolved matter (i.e., colloids) was more negative than particulate matter on the NF fouling for Al-hydroxide precipitate in presence of inorganic and organic matter.

**Keywords:** Al-hydroxide precipitate, Coagulation, Fouling, Nanofiltration

## 1. Introduction

Nanofiltration (NF) offers an attractive approach to meet multiple water quality objectives, such as removal of organic, inorganic, and microbial contaminants, and thus is a potential alternative to conventional water treatment [1-7]. Also, compared to reverse osmosis (RO) membrane, NF have operational advantages such as lower trans-membrane pressure (TMP), high flux, high retention of multivalent anion salts, an organic molecular weight above 300 Da, relatively low investment, and low operation and maintenance costs [8]. Because of these advantages, applications of NF to treat drinking water have increased in recent years motivated in part by stringent drinking water regulations. The world's largest NF plant with a capacity of 1,400,000  $\text{m}^3/\text{day}$  is situated in Mis-sur-Oise, close to Paris, France. It provides a population of about 800,000 inhabitants, in the north-west suburbs of Paris with high quality drinking water. The feed water to the NF is pre-treated water from the river Oise [9].

Coagulation as pretreatment to low pressure membrane such as microfiltration (MF) and ultrafiltration (UF) have been suggested to enhance membrane performances by removing par-

ticulates, colloidal matter, and particularly, organic compounds, i.e., natural organic matter (NOM) [10-14]. Therefore, coagulation can be used as pretreatment to salt rejecting membranes such as NF and RO which are more vulnerable in colloid and NOM fouling than in the low pressure membranes.

The system used for coagulation pretreatment could be designed with two different trains for membrane filtration. One is coagulation, flocculation, and either sedimentation or filtration to remove aggregates, i.e., floc followed by membrane filtration. Another one is coagulation and then membrane filtration where aggregates are included within feed water of membrane system. Comparing these two trains, it might be expected that the latter method is more appropriate to operate membrane system due to the reduced foot print, complexity, and operational costs.

However, in both pretreatment methods, the aggregate could be one of the major foulants for NF and RO membrane systems. Especially, aluminum (Al) residue in feed water resulting from the poor coagulation treatment can be transformed to Al-hydroxide precipitate as Al residue is influenced by various reaction conditions such as pH and temperature at the membrane surface and/or pores. Waite [15] also mentioned that polymeric

© This is an Open Access article distributed under the terms of the Creative Commons Attribution Non-Commercial License (<http://creativecommons.org/licenses/by-nc/3.0/>) which permits unrestricted non-commercial use, distribution, and reproduction in any medium, provided the original work is properly cited.

Received March 30, 2011 Accepted July 25, 2011

<sup>†</sup>Corresponding Author

E-mail: [jhkweon@konkuk.ac.kr](mailto:jhkweon@konkuk.ac.kr)

Tel: +82-2-450-4053 Fax: +82-2-454-4056

Al species with high molecular weight would accumulate at the membrane surface and lead, eventually, to precipitation of an aluminum hydroxide solid.

A hybrid membrane treatment system composed of low pressure membrane and coagulation pretreatment process has become of great interest since it is expected to provide better operation efficiencies [14, 16, 17]. Fouling, however, may become worse due to the floc formed in the coagulation pretreatment process, thus the fouling has been known as the greatest problem in the hybrid membrane process. It has reported that membrane fouling is closely related to the chemical, physical, and morphological properties of the floc which are dependent upon the solute water chemistry, primary particle size in raw water, and coagulation conditions [18-20]. Recently, Listiarini et al. [21] also argued that compared to larger pore membranes, i.e. MF and UF, NF membranes, suffer little or no pore blocking and thus there are possibilities of employing hybrid coagulation-nanofiltration technology for membrane treatment.

Some researchers have reported that the use of coagulation pretreatment causes an undesirable effect which is the presence of Al on NF and RO membrane performance [22-24]. Kim et al. [22] observed when employing three different NF pretreatment processes, the ratios of inorganic foulants to the total amounts of foulants are in the sequence of coagulation, sedimentation, and sand filtration water > MF water > Raw water, and in this case the major foulants are iron, silicate, calcium, potassium and aluminum. Park et al. [23] also detected inorganic foulants, i.e., Al and Si, on the fouled NF membrane surfaces and/or pores when different feed waters pretreated by coagulation/sedimentation and sand filtration were used. Additionally, Ohno et al. [24] reported that although the aluminum concentration in the NF feed was not high (30 µg/L), foulants can still accumulate an excess amount of aluminum and silicate, suggesting possible membrane fouling caused by alumino-silicates or aluminum hydroxide.

However, there are still not sufficient studies on the applications of coagulation pretreatment utilizing NF membrane system. Especially, the effectiveness of pretreatment with and without particulate matter, i.e., Al-hydroxide precipitate, was not evaluated. Thus, the objective of this paper is to investigate the Al-hydroxide precipitate fouling on the NF membrane performance such as permeability and rejection. Additionally, fouling of Al-hydroxide precipitate was observed in presence of organic compound, inorganic compound, and their combination. To understand the effect of particulate matter on the NF membrane, MF pretreatment was conducted before any NF experiment. The mathematical fouling model was also adapted to describe the mechanisms of membrane fouling.

## 2. Materials and Methods

### 2.1. Preparation of Al-hydroxide Precipitates

Polyaluminium chloride coagulant (PACl; 17% Al<sub>2</sub>O<sub>3</sub>; Yun Hap Chemical Industry Co., Ltd., Commercial grade, Incheon, Korea) was employed to form Al-hydroxide precipitate, i.e., floc. The PACl coagulant was then diluted to 1.0, 2.0, and 4.0 mM before performing any experiments.

1.0 M NaOH (Showa, Tokyo, Japan) was added to each Al solutions to adjust the pH in the range from 6.0 to 7.0, which is the desirable condition for Al-hydroxide formation since this

is suggested by the theoretical calculations using the solubility product constant [25].

Samples were taken without settling, filtered through a 0.45 µm polypropylene (PP) membrane filter (Whatman, Springfiled Mill, UK), and analyzed for the dissolved Al concentrations by atomic absorption spectrometer (AA6501F; Shimadzu, Kyoto, Japan).

Tap water was used in our study since it provided the solutions with both alkalinity and ionic strength representing natural waters with a low particle concentration. In addition, the tap water was available in a quantity that is sufficient for the continuous operation of filtration experiments together with the disposal of permeate and concentrate. Although the tap waters contain some dissolved chemical species such as Cl<sup>-</sup>, and SO<sub>4</sub><sup>2-</sup>, the interactions between Al and these species were not considered due to their the relatively low anion concentrations compared to the PACl dosage used in this study.

### 2.2. Addition of Inorganic or Organic Ingredient

CaCl<sub>2</sub>·2H<sub>2</sub>O (Showa, Tokyo, Japan) and MgSO<sub>4</sub>·7H<sub>2</sub>O (Showa, Tokyo, Japan) was used to investigate the influence of inorganic matter on Al-hydroxide fouling. The concentrations of the chemical solutions were prepared as 5.0 and 3.5 mM for Ca and Mg respectively in the NF experiments.

Humic acid solution used as the organic ingredient was prepared with Aldrich humic acid (Sodium salt, Aldrich, St. Louis, MO, USA) by dissolving 1 g of humic acid in 1 L of deionized water (PURELAB classic; ELGA LabWater, Lane End, UK), and filtering through a 0.45 µm membrane filter (Whatman, Springfiled Mill, UK). The humic acid solution was further diluted using tap water to approximately 10 mg/L as the dissolved organic carbon (DOC) and then applied to NF experiment.

### 2.3. NF membrane

Polypiperazine-amide thin-film composite NF membrane (Dow-Filmtec, Edina, MN, USA), which contains carboxylic and amine functional groups [26, 27], was used throughout the study. The NF membrane has, according to the manufacturer, replaced the discontinued NF 45 series and is primarily designed for process applications that require durable membranes. Also, the NF membrane is designed to remove organic matter with a molecular weight above 200 Da while passing monovalent salts and has a negatively charged surface between pH 4.2 to pH 11 within available operating pH conditions. The characteristics of the NF membrane used were summarized in Table 1.

### 2.4. NF Experiments

#### 2.4.1. Cross flow mode system

A schematic diagram of the NF apparatus is shown in Fig. 1. A plate-and-frame membrane module (Sepa-CF cell; Osmonics, Minnetonka, MN, USA) was used with a width of 0.095 m, a channel length of 0.146 m and an effective membrane surface area of 0.014 m<sup>2</sup>. A plastic sieve type feed spacer (Low foulant; Osmonics) stayed inside the cavity on the feeding side of the membrane. The NF membrane filtration system with a 4-L reservoir was operated within a constant pressure (approximately 490 kPa) using the high pressure pump (Wanner engineering, Minneapolis, MN, USA). The tap water with a flow rate of 1 L/min was gathered in the feed reservoir when PACl solution was

**Table 1.** Characteristics of NF membrane used in this study

Parameters	Physical and chemical properties
Membrane type	Polypiperazine-amide thin-film composite
Support material	PS <sub>s</sub> [28]
Surface material	PA <sub>p</sub> , TFC [28]
Molecular-weight cutoff (g/mol)	> 200
Salt rejection	Minimum 98% as 2,000 mg/L MgSO <sub>4</sub>
Isoelectric point (pH)	4.2 (this study), 5.1 [28]
Maximum operating temperature (°C)	45
Maximum operating pressure (psig)	600
Maximum pressure drop (psig)	15
Operating pH range	3-10
Free chlorine concentration (mg/L)	< 0.1
Pure water flux (L/m <sup>2</sup> ·hr·bar)	5.14 ± 0.51 (this study) 5.5 [29] 7.1 [30]

PS<sub>s</sub>: polysulphone, PA<sub>p</sub>, semi-aromatic piperazine-based polyamide, TFC: thin film composite.

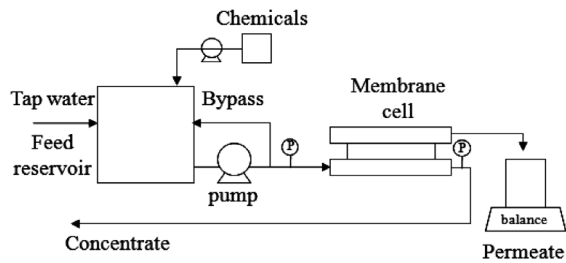


Fig. 1. Schematic diagram of cross flow nanofiltration (NF) systems.

injected at 3 mL/L simultaneously to adjust the Al concentration of feed water, i.e., 3.5 mM. The feed water pressurized at a flow rate of 0.5 L/min was compressed into the membrane module when the cross flow velocity was 0.9 m/sec on the membrane surface. The filtrate is measured continuously with an electronic balance (AND; Cole-Parmer International, Vernon Hills, IL, USA) to obtain data on the flux decline behaviour. The NF was stabilized overnight with deionized waters. At the start of each run, the membrane permeability was first determined with deionized waters.

#### 2.4.2. Dead-end mode system

The effectiveness of the coagulation pretreatment with and without particulate matter, i.e., Al-hydroxide precipitate, was evaluated by a microfilter (0.45 µm, PORPES; Chungsoo Technofil, Guro, Seoul, Korea) that removes particulate matter prior to each NF experiment. Dead-end filtration was employed due to the limited volume of feed water for the NF experiment. Dead-end NF filtrations were conducted using batch cells (180-mL capacity; Millipore, Billerica, MA, USA). Each cell was pressurized with a nitrogen gas at 40 ± 0.05 psi using a pressure controller (CZ-68026-58; Cole-Parmer International). An electronic balance (AND; Cole-Parmer International) was used to measure the

permeate mass, which was then converted to the permeate volume based on the feed water density. NF membrane used in this system has a surface area of 32.2 cm<sup>2</sup>. The clean water flux was determined for all fresh membranes using approximately 150 mL of deionized water. The experiment was terminated when the flux of feed water reached the steady state.

## 2.5. Application of Mathematical Fouling Models

Mathematical fouling models have been developed to explain the permeate flux reduction in the cross-flow membrane operation [31, 32]. Jarusutthirak et al. [32] used the mathematical fouling models to determine the kinetics of membrane fouling and to describe the fouling behaviours during NF as follows:

$$\frac{dJ_v}{dt} = -k \cdot (J_v - J^*) \cdot J_v^{2-n} \quad (1)$$

where  $J_v$  is the solution (permeate) flux;  $J^*$  is the solution flux associated with the back-transport mass transfer;  $k$  is the rate constant or fouling coefficient;  $t$  is the operating period; and  $n$  is a dimensionless filtration constant that expresses the specific fouling mechanism. The value of  $n$  depends on the model adapted in the calculation: for cake formation,  $n = 0$ ; for intermediate blocking,  $n = 1$ ; for pore constriction or standard blocking model,  $n = 1.5$ ; and for complete pore blocking,  $n = 2$ . Pore and intermediate blocking arises when foulants are similar in size to the pore diameter and hence results in severe flux decline. Pore constriction is caused by adsorption of foulants on the membrane walls. Foulants with sizes greater than a membrane pore diameter are rejected and consequently form a cake layer on the membrane surface. The term  $J^*$  in the equations was considered to be a critical flux, below which severe and rapid flux decline could be avoided, namely, a decline of flux did not occur [31]. The mathematical models describing the different fouling mechanisms are summarized in Table 2.

**Table 2.** Summary of fouling mechanisms and equations in the model

Fouling mechanisms	Equations
Pore blocking	$\frac{dJ_v}{dt} = -\frac{\alpha_{block} A_m C_{bulk} J_o}{n_o} (J_v - J^*) = -k_A (J_v - J^*)$
Pore constriction	$\frac{dJ_v}{dt} = -\frac{(2\alpha_{pore} A_m C_{bulk} J_o)^{0.5}}{\pi r_o^2 \delta_m} (J_v^{0.5} - J^*) = -k_B J_v^{0.5} (J_v - J^*)$
Intermediate blocking	$\frac{dJ_v}{dt} = -\frac{\alpha_{cake} R_c}{(R_m + R_c) \delta_c} A_m C_{bulk} J_o (J_v - J^*) = -k_C J_v (J_v - J^*)$
Cake formation	$\frac{dJ_v}{dt} = -\frac{\alpha_{cake} C_{bulk}}{R_m J_o} J_v^2 (J_v - J^*) = -k_D J_v^2 (J_v - J^*)$

## 2.6. Analytical Methods

The divalent cation was analyzed using an atomic absorption spectrometer (AA6501F; Shimadzu). The Al standard solution (Showa Chemical Co., Ltd., Kasugai, Japan) was used to obtain an Al standard curve before each analysis. DOC was measured using a Sievers 5310C Laboratory Total Organic Carbon Analyzer (GE Analytical Instruments Inc., Boulder, CO, USA) equipped with a 900 Autosampler System (Ionics Instruments, Boulder, CO, USA). Potassium hydrogen phthalate (Junsei Chemical Co., Ltd., Tokyo, Japan) was used as an external standard for DOC analysis. DOC measurements were taken after filtering the samples through the pre-rinsed 0.45 μm membrane syringe filters. A Hach 2100N turbidimeter (Hach, Loveland, CO, USA) was used to measure turbidity and a StablCal® Calibration Set was used for calibration. pH was measured using an Orion Model 410A pH meter (Thermo Electron Co., Beverly, MA, USA).

## 3. Results and Discussion

### 3.1. NF of Al-hydroxide Precipitate

#### 3.1.1. Feed water properties

The PACl solutions with three different Al concentrations were adjusted to pH neutral in order to observe the influence of Al-hydroxide precipitate on the NF membrane performance. Al-hydroxide precipitate was formed when the pH of feed waters were adjusted within the range 6.2 to 6.7. Properties of the three feed waters are included in Table 3. Compared to tap water (i.e., background water employed in this experiment), turbidity was not only highly increased approximately from 0.05 to 57.7 NTU but was also related to the increases in the total Al con-

**Table 3.** Characteristics of Al-hydroxide solutions with different Al concentrations

Parameters	Feed I	Feed II	Feed III
Temperature (°C)	21.9	21.6	20.7
pH (-)	6.7	6.2	6.4
Total Al (mM)	0.7	1.3	3.6
Conductivity (μS/cm)	334	462	832
Turbidity (NTU)	34.5	45.8	57.7

centrations at different feed waters. For instance the turbidities were 34.5, 45.8, and 57.7 NTU that correspond to Feed I, Feed II, and Feed III, respectively. A considerable quantity of particulate matter was Al-hydroxide precipitate such as Al(OH)<sub>3</sub>. The conductivity of the solutions was also increased due to the relatively large dosage of PACl used for Al concentration adjustment and NaOH for pH controlling from Feed I to Feed III.

#### 3.1.2. Evaluation of NF performance

In general, the flux decline and rejection rate are tools used to evaluate the membrane performance. As one of the parameters, the behavior of flux decline was applied to investigate the impact of Al-hydroxide precipitate with different Al concentrations on NF membrane fouling. The permeate flux was defined as the permeate volume per unit membrane area during a certain filtration time. The specific flux is result when the permeate flux was divided by the trans-membrane pressure. When the permeate and/or specific flux was divided by the initial flux, a normalized flux could be obtained. The normalized flux is useful to compare the flux decline behaviors of solutions with different initial flux values. For each set of experiments, the flux decline is presented in two different forms, namely the specific flux (Fig. 2a) and the corresponding normalized flux (Fig. 2b).

In fact, a significant flux decline under the impact of Al-hydroxide was expected possibly due to the accumulation of particulate matter with high turbidity on the membrane surface. However, during the NF experiments, little flux decline was observed. Moreover, the Al concentrations showed no considerable effect on membrane fouling even at high turbid concentrations, i.e., from 34.5 to 57.7. This indicates that both the Al and particulate matter concentrations were not important factors to NF membrane fouling. The fouling phenomenon therefore suggested that positively charged polymeric Al in the PACl solution would be neutralized by OH resulting in Al-hydroxide precipitate with no electrical surface charge. As a result, Al-hydroxide fouling with little flux decline was attributed to merely the accumulation of the precipitate with the abundant turbid matter on the membrane surfaces. Furthermore, it was reported that the amorphous Al-hydroxide can be formed with an OH/Al ratio of 3.0 [33]. Such amorphous precipitates might have a positive effect on the membrane fouling, possibly related to the formation of a porous and low resistant fouling layer without inner and/or external pore fouling at the membrane surface, which leads to the mitigation of severe membrane fouling.

To identify the accumulation of Al-hydroxide precipitate, the turbidity within the concentrate was measured during the NF

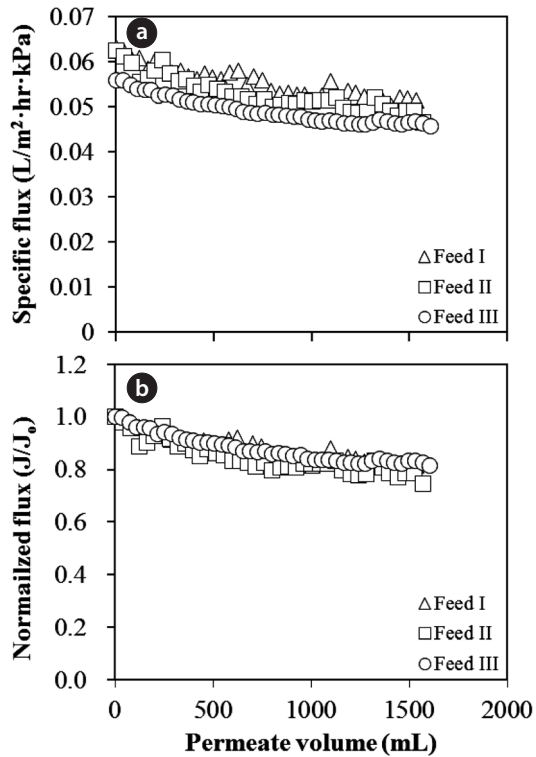


Fig. 2. Flux decline for Al-hydroxide precipitate fouling with different initial Al concentrations under neutral pH condition. (a) Specific flux and (b) Normalized flux. Operating conditions: TMP =  $509.4 \pm 7.5$  kPa; Cross flow velocity = 0.9 m/sec; Clean water flux =  $27.7 \pm 2.1$  LMH; Initial flux =  $29.1 \pm 2.2$  LMH.

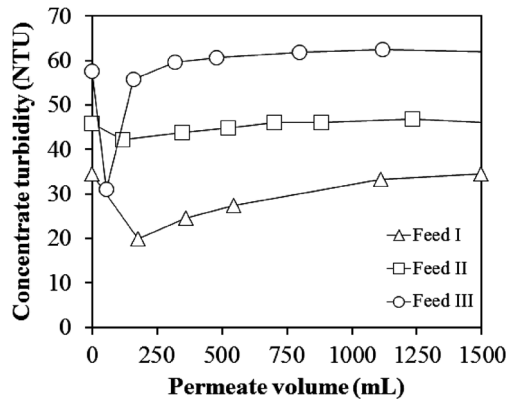


Fig. 3. Accumulation and repulsion of Al-hydroxide precipitate on the membrane surface: during nanofiltration (NF) experiment turbidity in concentrate disposed from cross flow NF membrane system with different Al concentration of feed waters.

experiment with different feed waters. As shown in Fig. 3, the turbidity was lowered at the initial period of membrane filtration, compared to the feed water. This result illustrated that the Al-hydroxide precipitate was accumulated on the membrane surface at the start of the filtration and also reveals that the cross flow velocity of 0.9 m/sec applied in this NF experiment was not a crucial factor to control the deposition of the precipitate on

the membrane. The turbidity was then gradually increased and reached a constant value close to the feed water turbidity. After which, the accumulation of Al-hydroxide on the membrane surface was thought to be limited.

Consequently, coagulation pretreatment without settling could be employed in a NF membrane system since the impact of the coagulated flocs was not significant on the NF membrane fouling. Listiarini et al. [21], also argued that compared to the larger pore membranes, i.e., MF and UF, NF membranes experience little or no pore blocking and thus there are possibilities of employing hybrid coagulation-nanofiltration technology in the removal of organic matter.

Other parameters used to evaluate the membrane performance are the rejection characteristic of Al and the conductivity during Al-hydroxide precipitate filtration with NF membrane. The permeate quality and rejection is presented in Table 4.

Most of the Al was rejected on the NF membrane regardless of the Al concentration of feed waters, since the Al rejection was 99.95% at 0.7 mM Al (Feed I), 98.89% at 1.3 mM Al (Feed II), and 100% at 3.6 mM Al (Feed III). Unlike the Al rejection, conductivity rejection was significantly lower at 29.5%, 13.8%, and 30.9% for Feed I, feed II, and Feed III, respectively.

As described in the literature, the surface charge of NF membrane plays a critical role in the rejection of charged ion [8, 34, 35]. It is briefly summarized as the electrostatic repulsion, i.e., Donnan exclusion, between the charged ion and membrane surface. Therefore, the conductivity rejection might be rationalized as the cake layer accumulated by Al-hydroxide precipitate which shielded the negative charge of membrane at the neutral pH condition and consequently caused weak repulsion forces between the membrane and the charged ion.

Gabelich et al. [36] also reported that the salt rejection was decreased in RO membrane systems with coagulation pretreatment using PACl coagulant, in which the residual Al concentration was 50  $\mu\text{g/L}$  at ambient pH conditions (pH 7.8-7.9). Additionally, Schrader et al. [37] suggested that the decrease in salt rejection as a result of the Al addition to the feed water at pH 8.0 led to a decreased membrane surface potential, i.e., the loss of electrostatic repulsion.

### 3.2. Influence of Inorganic and Organic Matter

To compare the effect of different compounds on Al-hydroxide precipitate fouling, the normalized flux decline for the fouling in presence of Ca, Mg, humic acid, and their combination, i.e., Mg and humic acid, were presented in Fig. 4 where for all three cases the flux decline rates were increased.

Overall the flux decline rate was only slightly increased in presence of humic acid. It is postulated that the increased resis-

Table 4. Characteristics of rejection and permeate water quality for Al-hydroxide fouling

Parameters		Feed I	Feed II	Feed III
Permeate	Al (mM)	0.0004	0.01	N/D
	Conductivity ( $\mu\text{S/cm}$ )	235.4	398.4	575.0
Rejection (%)	Al	99.9	98.9	100.0
	Conductivity	29.5	13.8	30.9

N/D: not detected.



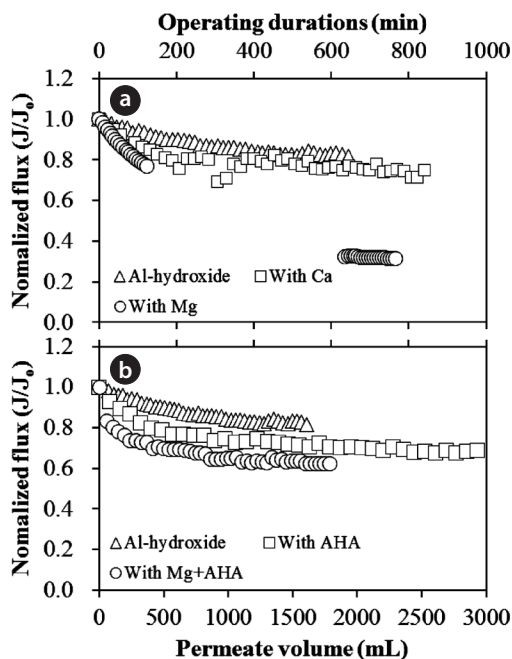


Fig. 4. Normalized permeate flux decline for the Al-hydroxide precipitate fouling in presence of (a) organic and (b) inorganic and their combination. Operating conditions: TMPs = 513.9 ± 16.6 kPa; Cross flow velocity = 0.9 m/sec; Clean water flux = 21.7 ± 3.8; Initial flux = 22.0 ± 6.1 LMH.

tances of cake layer formed by Al-hydroxide in presence of humic acid results in a more decreased flux decline rate compared to the Al-hydroxide precipitate fouling without humic acid. It is also noted that the high humic water flocs (i.e., Al-hydroxide precipitate) were more compressible under external pressures, which can substantially increase the cake resistance [38].

The impact of the divalent cation on Al-hydroxide precipitate fouling was more substantial in presence of Mg than Ca. This shows that the impact of Mg on the increase of the cake layer resistance was more significant than Ca. Additionally, the flux decline with Al-hydroxide precipitate and humic acid was further reduced by introducing Mg into the solution. This suggests that the resistance of the combined cake layer formed by Al-hydroxide and humic acid could be further enhanced in presence of Mg. In the previous study on organic fouling of loose NF membranes [39], Mg have been shown to increase the organic fouling rate attributed to the electrostatic interaction with NOM. However the effect of which was not as significant when compared to Ca due to an intermolecular bridging mechanism. On comparison, the intermolecular bridging mechanism of Ca found in organic fouling was not significant in presence of colloidal matter [40].

At the Al-hydroxide precipitate fouling on the NF membrane, Mg dramatically reduced the flux decline of the initial water specific flux by 68.4% compared to 37.6% of initial water specific flux with Mg and humic acid after a permeate volume of approximately 3,500 mL. Unlike the negative effect of Mg on the Al-hydroxide precipitate fouling, humic acid played a critical role in the release of the suggested resistance of the cake layer formation along with Mg despite the membrane fouling for Al-hydroxide alone could be further deteriorated in presence of Mg

and humic acid, possibly due to different cake properties.

The rejection feature of the NF membrane was observed for Al-hydroxide precipitate fouling in presence of inorganic compound, organic compound, and their combination. As shown in Table 5, the Al rejection was more than 99.9%, which demonstrated the high Al selectivity of the membrane. However, as discussed above, the charge of the membrane surface may have been neutralized, due to the accumulation of the Al-hydroxide precipitate, resulting in the increased ion transport through the NF membrane without electrostatic repulsion.

Moreover, the rejection of conductivity was 3.2 to 61.2% at each experiment system. Of which the humic acid was a significant factor decreasing the conductivity rejection by 3.2%. It should be noted that humic acid in feed water was primarily controlled to prevent the deteriorating removal of conductivity for Al-hydroxide precipitate fouling in coagulation followed by NF membrane system. In addition, even though a low DOC concentration due to the removal of DOC by Al-hydroxide precipitate is introduced to the membrane, relatively low DOC rejection of 25.0% was observed in presence of humic acid. However, when both Mg and humic acid were added to the solution of Al-hydroxide precipitate, the rejection of DOC and conductivity was increased by 68.6 and 61.2%, respectively.

### 3.3. Influence of MF Pretreatment

Effect of the MF membrane pretreatment on NF membrane fouling by Al-hydroxide precipitate was investigated. Interestingly, Fig. 5 shows that the MF membrane pretreatment did not mitigate the Al-hydroxide precipitate fouling but increased the rate of flux decline. The negative effect of MF membrane pretreatment was most severe for feed water with Al-hydroxide precipitate alone. This result suggests that the dissolved matter with size of 0.45 μm below were major foulants such as colloids for Al-hydroxide precipitate fouling on NF membrane with MF membrane pretreatment. In fact, a significant impact of Al-hydroxide precipitate on NF membrane might be expected possibly due to the formation of fine particles.

Bertsh et al. [41] suggested that fine particulate matter such as colloidal solids could be formed at the initial coagulation reactions and also Pernitsky and Edzwald [25] mentioned that microcrystall particles with a size range of 1 nm to 200 nm could be formed when PACl was used for coagulation treatment. Inversely, it is worth to note that the particulate matter may also contribute to the mitigation of the dissolved matter fouling even though the mechanism of fouling reduction proposed in this paper could not rationalize this.

Table 5. Rejection characteristic for Al-hydroxide precipitate fouling in presence of organic compound, inorganic compound, and their combination

System	Rejection (%)				
	Al	Ca	Mg	DOC	Conductivity
With Ca	99.9	32.8	- <sup>a</sup>	-	24.9
With Mg	N/D	-	75.8	-	40.5
With humic acid	N/D	-	-	25.0	3.2
With Mg and humic acid	N/D	-	65.2	68.6	61.2

DOC: dissolved organic carbon, N/D: not detected.

<sup>a</sup> - denotes that compound was not added into the feed solution.

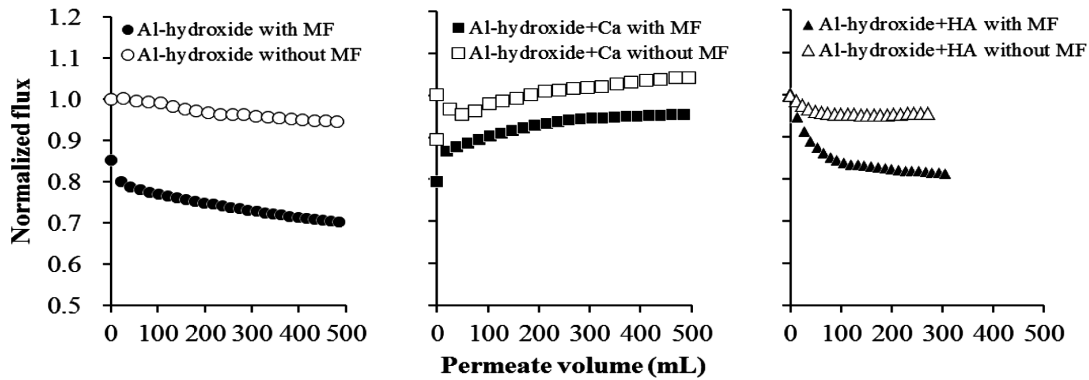


Fig. 5. Normalized permeate flux decline for the Al-hydroxide precipitate fouling in presence of organic and inorganic matter with and without MF pretreatment. Operating conditions: TMPs = 275.8 kPa; Cross flow velocity = 0 m/sec; Clean water flux =  $13.9 \pm 1.34$  LMH; Initial flux =  $13.0 \pm 2.0$  LMH.

Table 6. Variable fouling mechanisms and critical flux calculated from mathematical model for combined Al species fouling

System	Fouling ratio <sup>a</sup>	Fouling mechanism	Fouling coefficient ( $\text{hr}\cdot\text{m}^{-2}$ )	Critical flux ( $\text{L}/\text{m}^2\cdot\text{hr}$ )	SSE
Al-hydroxide	18.3	Cake formation	$8.74 \times 10^{-4}$	23.8	1.57
With Ca	25.4	Cake formation	$7.44 \times 10^{-4}$	18.6	81.2
With Mg	68.4	Cake formation	$2.09 \times 10^{-4}$	N/A	20.7
With HA	33.6	Cake formation	$7.33 \times 10^{-4}$	18.2	9.73
With Mg and HA	37.6	Cake formation	$3.10 \times 10^{-3}$	8.76	6.95

SSE: sum of squared errors.

<sup>a</sup>% of clean water flux.

Al-hydroxide fouling both with and without MF membrane pretreatment was reduced in the presence of Ca while a significant flux decline rate at initial stage of NF operation was gradually increased to the initial membrane flux during the NF membrane experiment. Different from the result at the cross flow system, the operating condition, i.e., cross flow and/or dead-end mode, of the NF membrane system could affect the role of Ca on Al-hydroxide fouling, postulated to the different fouling mechanism.

In summary, MF membrane pretreatment revealed negative effects on NF membrane fouling of Al-hydroxide precipitate in presence and absence of Ca and humic acid. The flux decline rate of the feed waters with the MF membrane pretreatment was increased more than the one without the MF pretreatment. The results suggest that the “dissolved” species such as colloids participated in the membrane fouling in a greater extent than particulate matter for Al-hydroxide precipitate. Most of the NF membrane experiments in this study did not employ pretreatment such as settling and/or filtration of feed waters. The installation of a filter such as cartridge filter, microfiltration, or ultrafiltration, is recommended to protect the high pressure pumps for NF in real plants. However, results presented here suggest that the installation did not reduce NF fouling.

### 3.4. Fouling Mechanism

The models proposed by Jarusutthirak et al. [32] were used to estimate the fouling mechanisms associated with Al-hydroxide

precipitate. Table 6 presents the calculated parameters from the fouling model with fouling ratio presented above results. These results were based on minimizing the sum of squared errors (SSE) between the experimental data and the estimated data from each of the fouling models ( $\sum [J_v(\text{model}) - J_v(\text{measured})]^2$ ). The model with the smallest SSE could be considered as a more accurate fit, and thus a more feasible fouling mechanism for a given solution.

Of which, the cake formation mechanism was the best fit. This therefore indicates that the Al-hydroxide precipitate larger than the pore size of the NF membrane was apparently accumulated on the membrane surfaces resulting in formation of cake layer. Also, this results support the formation of a porous and low resistant fouling layer without inner and/or external pore fouling at the membrane surface, which avoids severe membrane fouling. However, when the same fouling mechanism was adapted for different feed waters, the behavior of membrane fouling was varied in the range of 18.3 to 68.4% as a fouling ratio. Such variations might be attributed to certain properties of the cake layer on the membrane surfaces such as specific cake resistance and compressibility [1].

The critical flux,  $J^*$ , associated with the back-transport mass transfer is applied to compare the Al-hydroxide precipitate fouling with and without organic, inorganic, and their combination. The critical flux depends on the hydrodynamics, physicochemical properties of feed water, and other variables. If feed waters has a greater critical flux, the system can be operated with higher flux and therefore possess less tendency of fouling. As shown in

Table 6, the critical flux was the smallest for the Al-hydroxide precipitate solution together with Mg and humic acid.

This indicates that the Al-hydroxide precipitate fouling was most severely occurred in presence of Mg and humic acid simultaneously, but the significant flux decline might be avoided when NF membrane system was operated approximately 8.8 LMH below initial flux.

In addition, the fouling mechanisms of Al-hydroxide with and without Mg and humic acid are suggested to be the same as cake formation but with more flux decline rate when both Mg and humic acid are present. The  $K_D$  ( $\text{h}\cdot\text{m}^{-2}$ ) which indicates the rate constant or fouling coefficient for cake formation was calculated to be  $8.74 \times 10^{-4}$  and  $3.10 \times 10^{-3}$  for Al-hydroxide alone and in presence Mg and humic acid, respectively. This result agrees well with the increased cake resistance of Al-hydroxide resulting from the presence of Mg and humic acid on the membrane surfaces.

## 4. Conclusions

The Al-hydroxide precipitate fouling on the NF membrane performance was investigated in presence of organic compound, inorganic compound, and their combination. Also, the influence of MF on NF membrane system with coagulation pretreatment was evaluated. In particular, remarkable conclusions that can be drawn from this research are as follows:

- 1) Al-hydroxide precipitate had little effect on the NF membrane fouling with a low flux decline rate regardless of the particulates concentration, i.e., turbidity resulting from the increase in Al concentrations. Al-hydroxide precipitate accumulated on the membrane did form a cake layer which was one of the major factors avoiding severe flux decline.
- 2) The NF rejection of conductivity was significantly deteriorated by Al-hydroxide precipitate fouling. The cake layer led to weak repulsion forces between the membrane and the charged ionic contents.
- 3) Mg dramatically increased the Al-hydroxide precipitate fouling for NF. However, humic acid played a critical part in the resistance reduction of the cake layer formed by Al-hydroxide along with Mg. It is most likely that the fouling with inorganic compounds relies on the presence and absence of organic matter possibly due to different cake properties.
- 4) The Al-hydroxide precipitate may contribute heavily to the mitigation of dissolved matter fouling and therefore coagulation without settling and/or prefiltration could be used as a pretreatment method for the NF membrane systems.

## Acknowledgments

This research was supported by Basic Science Research Program through the National Research Foundation of Korea (NRF) funded by the Ministry of Education, Science and Technology (531-2006-1-D00011).

## References

1. Lee S, Lee CH. Effect of operating conditions on  $\text{CaSO}_4$  scale formation mechanism in nanofiltration for water softening. *Water Res.* 2000;34:3854-3866.

2. Tay JH, Liu J, Delai Sun D. Effect of solution physico-chemistry on the charge property of nanofiltration membranes. *Water Res.* 2002;36:585-598.
3. Kilduff JE, Mattaraj S, Belfort G. Flux decline during nanofiltration of naturally-occurring dissolved organic matter: effects of osmotic pressure, membrane permeability, and cake formation. *J. Membr. Sci.* 2004;239:39-53.
4. Koyuncu I, Topacik D, Wiesner MR. Factors influencing flux decline during nanofiltration of solutions containing dyes and salts. *Water Res.* 2004;38:432-440.
5. Bodzek M, Koter S, Wesolowska K. Application of membrane techniques in a water softening process. *Desalination* 2002;145:321-327.
6. Lin CJ, Shirazi S, Rao P, Agarwal S. Effects of operational parameters on cake formation of  $\text{CaSO}_4$  in nanofiltration. *Water Res.* 2006;40:806-816.
7. Nanda D, Tung KL, Hsiung CC, et al. Effect of solution chemistry on water softening using charged nanofiltration membranes. *Desalination* 2008;234:344-353.
8. Hilal N, Al-Zoubi H, Darwish NA, Mohammad AW, Abu Arabi M. A comprehensive review of nanofiltration membranes: treatment, pretreatment, modelling, and atomic force microscopy. *Desalination* 2004;170:281-308.
9. Wittmann E, Thorsen T. Water treatment. In: Schaefer AI, Fane AG, Waite TD, eds. *Nanofiltration: principles and applications*. Oxford: Elsevier Advanced Technology; 2007. Ch. 10. p. 273-284.
10. Vickers JC, Thompson MA, Kelkar UG. The use of membrane filtration in conjunction with coagulation processes for improved NOM removal. *Desalination* 1995;102:57-61.
11. Carroll T, King S, Gray SR, Bolto BA, Booker NA. The fouling of microfiltration membranes by NOM after coagulation treatment. *Water Res.* 2000;34:2861-2868.
12. Bérubé PR, Mavinic DS, Hall ER, Kenway SE, Roett K. Evaluation of adsorption and coagulation as membrane pretreatment steps for the removal of organic material and disinfection-by-product precursors. *J. Environ. Eng. Sci.* 2002;1:465-476.
13. Pikkariainen AT, Judd SJ, Jokela J, Gillberg L. Pre-coagulation for microfiltration of an upland surface water. *Water Res.* 2004;38:455-465.
14. Kim HC, Hong JH, Lee S. Fouling of microfiltration membranes by natural organic matter after coagulation treatment: a comparison of different initial mixing conditions. *J. Membr. Sci.* 2006;283:266-272.
15. Waite TD. Chemical speciation effect in nanofiltration separation. In: Schaefer AI, Fane AG, Waite TD, eds. *Nanofiltration: principles and applications*. Oxford: Elsevier Advanced Technology; 2007. Ch. 7. p. 166-167.
16. Park PK, Lee CH, Choi SJ, Choo KH, Kim SH, Yoon CH. Effect of the removal of DOMs on the performance of a coagulation-UF membrane system for drinking water production. *Desalination* 2002;145:237-245.
17. Oh JI, Lee S. Influence of streaming potential on flux decline of microfiltration with in-line rapid pre-coagulation process for drinking water production. *J. Membr. Sci.* 2005;254:39-47.
18. Cho MH, Lee CH, Lee S. Effect of flocculation conditions on membrane permeability in coagulation-microfiltration. *Desalination* 2006;191:386-396.
19. Jefferson B, Jarvis P, Sharp E, Wilson S, Parsons SA. Flocs through the looking glass. *Water Sci. Technol.* 2004;50:47-54.
20. Lee JD, Lee SH, Jo MH, Park PK, Lee CH, Kwak JW. Effect of



- coagulation conditions on membrane filtration characteristics in coagulation--microfiltration process for water treatment. *Environ. Sci. Technol.* 2000;34:3780-3788.
21. Listiari K, Sun DD, Leckie JO. Organic fouling of nanofiltration membranes: evaluating the effects of humic acid, calcium, alum coagulant and their combinations on the specific cake resistance. *J. Membr. Sci.* 2009;332:56-62.
  22. Kim HA, Choi JH, Takizawa S. Comparison of initial filtration resistance by pretreatment processes in the nanofiltration for drinking water treatment. *Sep. Purif. Technol.* 2007;56:354-362.
  23. Park N, Lee S, Yoon SR, Kim YH, Cho J. Foulants analyses for NF membranes with different feed waters: coagulation/sedimentation and sand filtration treated waters. *Desalination* 2007;202:231-238.
  24. Ohno K, Matsui Y, Itoh M, et al. NF membrane fouling by aluminum and iron coagulant residuals after coagulation-MF pretreatment. *Desalination* 2010;254:17-22.
  25. Pernitsky DJ, Edzwald JK. Solubility of polyaluminium coagulants. *J. Water Supply Res. Technol. Aqua* 2003;52:395-406.
  26. Schaep J, Vandecasteele C. Evaluating the charge of nanofiltration membranes. *J. Membr. Sci.* 2001;188:129-136.
  27. Her N, Amy G, Jarusutthirak C. Seasonal variations of nanofiltration (NF) foulants: identification and control. *Desalination* 2000;132:143-160.
  28. Tanninen J, Mänttari M, Nyström M. Effect of salt mixture concentration on fractionation with NF membranes. *J. Membr. Sci.* 2006;283:57-64.
  29. Bargeman G, Vollenbroek JM, Straatsma J, Schroën CGPH, Boom RM. Nanofiltration of multi-component feeds. Interactions between neutral and charged components and their effect on retention. *J. Membr. Sci.* 2005;247:11-20.
  30. Balannec B, Vourch M, Rabiller-Baudry M, Chaufer B. Comparative study of different nanofiltration and reverse osmosis membranes for dairy effluent treatment by dead-end filtration. *Sep. Purif. Technol.* 2005;42:195-200.
  31. Field RW, Wu D, Howell JA, Gupta BB. Critical flux concept for microfiltration fouling. *J. Membr. Sci.* 1995;100:259-272.
  32. Jarusutthirak C, Mattaraj S, Jiratananon R. Influence of inorganic scalants and natural organic matter on nanofiltration membrane fouling. *J. Membr. Sci.* 2007;287:138-145.
  33. Zelazny LW, Jardine PM. Surface reactions of aqueous aluminum species. In: Sposito G, ed. *The environmental chemistry of aluminum*. Boca Raton, FL: CRC Press; 1989. p. 149-155.
  34. Mänttari M, Pihlajamäki A, Nyström M. Effect of pH on hydrophilicity and charge and their effect on the filtration efficiency of NF membranes at different pH. *J. Membr. Sci.* 2006;280:311-320.
  35. Bouranene S, Fievet P, Szymczyk A, El-Hadi Samar M, Vidonne A. Influence of operating conditions on the rejection of cobalt and lead ions in aqueous solutions by a nanofiltration polyamide membrane. *J. Membr. Sci.* 2008;325:150-157.
  36. Gabelich CJ, Ishida KP, Gerringer FW, Evangelista R, Kalyan M, Suffet IHM. Control of residual aluminum from conventional treatment to improve reverse osmosis performance. *Desalination* 2006;190:147-160.
  37. Schrader GA, Zwijnenburg A, Wessling M. The effect of WWTP effluent zeta-potential on direct nanofiltration performance. *J. Membr. Sci.* 2005;266:80-93.
  38. Choi YH, Kim HS, Kweon JH. Role of hydrophobic natural organic matter flocs on the fouling in coagulation-membrane processes. *Sep. Purif. Technol.* 2008;62:529-534.
  39. Li Q, Elimelech M. Organic fouling and chemical cleaning of nanofiltration membranes: measurements and mechanisms. *Environ. Sci. Technol.* 2004;38:4683-4693.
  40. Li Q, Elimelech M. Synergistic effects in combined fouling of a loose nanofiltration membrane by colloidal materials and natural organic matter. *J. Membr. Sci.* 2006;278:72-82.
  41. Bertsh PM. Aqueous polynuclear aluminum species. In: Sposito G, ed. *The environmental chemistry of aluminum*. Boca Raton, FL: CRC Press; 1989. p. 107-109.